Rotational relaxation of molecular ions in a buffer gas

Jesús Pérez-Ríos[1,*] and F. Robicheaux[1,2]
[1]*Department of Physics and Astronomy, Purdue University, West Lafayette, Indiana 47907, USA*
[2]*Purdue Quantum Center, Purdue University, West Lafayette, Indiana 47907, USA*
(Received 4 August 2016; published 21 September 2016)

The scattering properties regarding the rotational degrees of freedom of a molecular ion in the presence of a buffer gas of helium are investigated. This study is undertaken within the framework of the infinite-order sudden approximation for rotational transitions, which is shown to be applicable to a large variety of molecular ions in a buffer gas of helium at fairly low temperatures. The results derived from the present approach have potential applications in cold chemistry and molecular quantum logic spectroscopy.

DOI: 10.1103/PhysRevA.94.032709

I. INTRODUCTION

The development of hybrid ion-neutral trap technology has revolutionized the field of cold chemistry, allowing the study of atomic ion-neutral chemical processes, such as charge exchange reactions [1–8], radiative association [1,2,4], and three-body recombination reactions [9]. However, driven by the possibility of state-selective chemistry [5,10], sympathetic cooling of trapped molecular ions [11–13], spectroscopy of buffer-gas-cooled trapped molecular ions [14], and molecular quantum logic spectroscopy [15–17], molecular ion-neutral collisions are becoming more relevant. In molecular ion-atom collisions the translational degrees of freedom are coupled to the internal states of the molecule (rotational, vibrational, and electronic) through the anisotropy of the potential energy surface (PES). As a consequence, atom-molecule collisions may induce changes in the internal quantum state of the molecule as sketched in Fig. 1 for the case of rotation. This process is the core of the thermalization mechanisms and transport in gases, known as relaxation phenomena [18–21]. Therefore, relaxation phenomena will play an important role in the control of internal degrees of freedom of molecular ions brought in contact with neutrals.

In principle, for low collision energies, $\sim$1 K, having the PES of the system under consideration, one could solve the Schrödinger equation by means of the coupled-channel (CC) method employing the PES, as Soecklin *et al.* [13] have recently accomplished for the study of vibrational quenching of molecular ions in the presence of a buffer gas, leading to accurate but computationally expensive results. For thermal energies of $\sim$300 K the problem is computationally intractable within the CC method due to the huge size of the Hilbert space needed to guarantee the convergence of the calculations. Nevertheless, it is possible to assume some approximation regarding the translation-rotation (TR) energy transfer which will simplify the theoretical treatment without loss of accuracy and predictive power, such as the coupled-states approximation [22,23] and the infinite-order sudden (IOS) approximation [24–28].

In this paper, a study of rotational relaxation for molecular ion-atom collisions relevant for cold chemistry experiments is presented. The scattering calculations are developed within the IOS framework. The atom-molecule interaction is characterized by a realistic anisotropic long-range potential, whereas the short range is treated through a model potential. The IOS approach is explained and its range of validity analyzed for a large number of molecular ion-atom collisions relevant for cold chemistry experiments.

The paper is structured as follows: in Sec. II, the inelastic rotational cross section within the IOS framework is introduced and its validity is studied for molecular ions relevant for atom-ion hybrid trap setups. In Sec. III, the IOS framework is applied to the study of rotational relaxation of molecular ions in a He buffer gas. In particular, results for MgH^+ and BaH^+ as examples of $^1\Sigma$-He and for SiO^+ as an example of $^2\Sigma$-He collisions are presented. In the same section the IOS approximation is tested against CC calculations for different molecular ions. Finally, in Sec. IV, the outlook and conclusions are presented.

II. INFINITE-ORDER SUDDEN APPROXIMATION

Let us assume a molecular ion-atom collision; we treat the molecular ion as a rigid rotor and the interaction potential between the colliding partners is fully specified by two degrees of freedom $V(R,\delta)$, where R is the distance between the atom and the center of mass (CM) of the molecular ion, i.e., the scattering coordinate, and δ stands for the relative angle between **R** and the rigid rotor as shown in Fig. 2. In the space-fixed (SF) frame of reference where the orientation of the rigid rotor is described as $\omega_{\rm SF} = (\theta_{\rm SF},\phi_{\rm SF})$ (see Fig. 2) and the relative orientation of the atom with respect to the CM of the molecular ion is $\omega_a = (\theta_a,\phi_a)$ (see Fig. 2), the scattering wave function is expressed as [29]

$$\Psi(\omega_{\rm SF},\omega_a,R) = \sum_{Nl\mathcal{J}M} \frac{u_{Nl}^{\mathcal{J}M}(R)}{R}\psi_{Nl\mathcal{J}M}(\omega_{\rm SF},\omega_a), \quad (1)$$

where the total angular momentum $\mathcal{J}$ and its projection onto the laboratory axis M are conserved quantities due to the absence of external fields, and

$$\psi_{Nl\mathcal{J}M}(\omega_{\rm SF},\omega_a) = \sum_{m_N m_l} C^{\mathcal{J}M}_{lm_lNm_N} Y_l^{m_l}(\omega_a) Y_N^{m_N}(\omega_{\rm SF}). \quad (2)$$

Here, $Y(\omega)$ represent the spherical harmonics, and in particular, $Y_N^{m_N}(\omega_{\rm SF})$ denotes the rotational wave function for the rigid rotor. By substituting Eq. (1) into the Schrödinger

*jperezri@purdue.edu

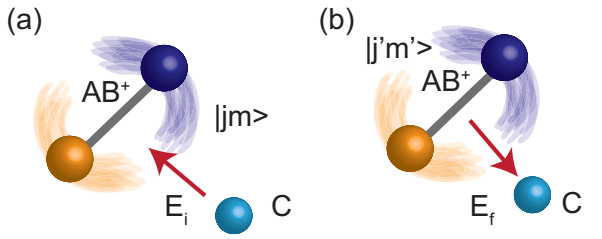

FIG. 1. Rotational relaxation mechanism. An atom C collides with a molecular ion AB^+ (assumed to be at rest, for simplicity) through the atom-molecule interaction. This interaction is responsible for the coupling between the rotational and the translational degrees of freedom. As a consequence, the molecule can be found in a different rotational state $|j'm'\rangle$ after the collision, but with the constraint $E_f + B_e j'(j'+1) = E_i + B_e j(j+1)$ due to the conservation of energy, where B_e is the rotational constant.

equation and neglecting the trivial motion of the center of mass CM, the u's are the solution of a set of coupled differential equations,

$$\left[\frac{d^2}{dR^2} - \frac{l(l+1)}{R^2} + k_N^2\right] u_{Nl}^{\mathcal{J}M}(R) = 2\mu \sum_{N'l'} \langle Nl\mathcal{J}M|V(R,\delta)|N'l'\mathcal{J}M\rangle u_{N'l'}^{\mathcal{J}M}(R), \quad (3)$$

where $k_N^2 = 2\mu(E - B_e N(N+1))$, E denotes the available precollision relative total energy of the molecular ion-atom system, and hence the collision energy is $E_k = k_N^2/(2\mu)$. μ is the reduced mass for the molecular ion-atom system and B_e is the rotational constant of the molecular ion. The solution of Eq. (3) with the appropriate boundary conditions leads to the rotational relaxation cross section, which is the result of an intricate interplay between the relative angular momentum l and the rotational state of molecule N through the PES $V(R,\delta)$. However, this complexity can be reduced by assuming that N and l are decoupled, as shown below.

The PESs for different molecular ion-atom collisions have been calculated by means of a model potential at short range, whereas the long-range tail of the atom-molecule interaction is modeled by the isotropic charge-neutral interaction $\propto R^{-4}$ and the anisotropic induced dipole-charge interaction $\cos(\delta)R^{-5}$,

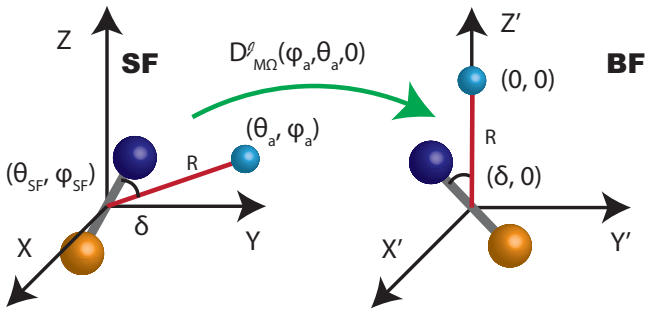

FIG. 2. Space-fixed (SF) frame (X,Y,Z) and body-fixed (BF) frame (X',Y',Z') of reference for atom-molecule collisions. Transformation from one system into the other through the Wigner D matrix $D^{\mathcal{J}}_{M\Omega}(\phi_a,\theta_a,0)$ is possible, as explained in the text.

yielding (in atomic units)

$$V(R,\delta) = -\frac{\alpha}{2R^4}\left[1 - \frac{1}{2}\left(\frac{R_m}{R}\right)^4\right] + \frac{2d\alpha\cos(\delta)}{R^5}, \quad (4)$$

where α is the polarizability of the atom, d is the permanent dipole moment of the molecular ion, and R_m stands for the position of the minimum of the well. R_m only affects the short-range physics of the molecular ion-atom interaction, and since the anisotropy of the interaction is due to the long-range tail of the PES, R_m will not play a role in the rotational relaxation.

McGuire and Kouri pointed out that effects of the couplings between l and N are better studied in a system of reference attached to the molecular ion-atom system [22,23], the so-called body-fixed (BF) frame, as displayed in Fig. 2. This reference frame is related to the SF by means of the Wigner D rotation matrix $D^{\mathcal{J}}_{M\Omega}(\theta,\beta,0)$, where (θ,β) represent the Euler angles. In the BF frame the solution of the Schrödinger equation leads to

$$\left[\frac{d^2}{dR^2} + k_N^2\right] u_{N\Omega}^{JM}(R) = \langle N\Omega\mathcal{J}M|\frac{\hat{\mathbf{l}}^2}{R^2}|N'\Omega'\mathcal{J}M\rangle u_{N'\Omega'}^{\mathcal{J}M}(R) + 2\mu \sum_{N'\Omega'} \langle N\Omega\mathcal{J}M|V(R,\delta)|N'\Omega'\mathcal{J}M\rangle u_{N'\Omega'}^{\mathcal{J}M}(R), \quad (5)$$

where

$$|N\Omega M\rangle = \sqrt{\frac{2\mathcal{J}+1}{4\pi}} D^{\mathcal{J}*}_{M\Omega}(\phi_a,\theta_a,0) Y_N^{m_N}(\delta,0), \quad (6)$$

and Ω represents the projection of N onto the molecular axis. In Eq. (5) the potential $V(R,\delta)$ only couples states with the same projection Ω, whereas the $\hat{l}^2$ operator couples states with different Ω's; this is the so-called Coriolis coupling [22,23,28,30]. At high collision energies, as well as for systems where the anisotropy associated with the atom-molecule energy landscape is low, the Coriolis coupling may be neglected. This is the so-called centrifugal decoupling or coupled-states approximation [22,23]. In this approximation the relative motion in the molecular ion-atom system cannot induce any change in Ω; as a consequence, only the diagonal terms of $\langle N\Omega\mathcal{J}M|\frac{\hat{\mathbf{l}}^2}{R^2}|N'\Omega'\mathcal{J}M\rangle$ play a role.

In the IOS approximation molecular ion-atom collisions are assumed to occur on a time scale such that the molecular ion does not rotate significantly during the encounter; thus apart from neglecting the Coriolis coupling, it is reasonable to solve Eq. (5) with δ as a parameter and with a collision energy independent of the initial state of the molecule, i.e.,

$$\left[\frac{d^2}{dR^2} - \frac{l(l+1)}{R^2} + k^2 - 2\mu V(R,\delta)\right] f(k,R) = 0, \quad (7)$$

The solution must satisfied the boundary conditions $f(k,R) \to 0$ for $R \to 0$, but as $R \to \infty$,

$$f(k,R) \sim \frac{1}{\sqrt{k}}(e^{-\imath(kR - \frac{l\pi}{2})} - S^l(k,\delta)e^{\imath(kR-\frac{l\pi}{2})}), \quad (8)$$

where $S^l(k,\delta)$ represents the S matrix for a given δ and wave vector $k = \sqrt{2\mu E}$. Once $S^l(k,\delta)$ is known, the rotational

relaxation cross section can be calculated, however, some special care needs to be taken in terms of the kind of molecule at hand, as shown below.

A. $^1\Sigma$ molecular ion-atom collisions

For the case of $^1\Sigma$ molecules the rotational quantum number N is a good quantum number due to the absence of spin. Thus, by means of $S^l(k,\delta)$, the S matrix linking two rotation states, N and N', is calculated as

$$S^l_{N\Omega;N'\Omega}(k) = \langle N\Omega|S^l(k,\delta)|N'\Omega\rangle \tag{9}$$

$$= 2\pi \int_0^\pi Y_N^{*\Omega}(\delta,0) S^l(k,\delta) Y_{N'}^{\Omega}(\delta,0) \sin\delta d\delta, \tag{10}$$

and the rotational relaxation cross section in the IOS approach is given by [28,30]

$$\sigma_{N\to N'}(k) = \sum_l \sigma^l_{N\to N'}(k)$$

$$= \frac{\pi}{(2N+1)k^2} \sum_{l\Omega} (2l+1)|S^l_{N\Omega;N'\Omega}(k)|^2, \tag{11}$$

with $N \neq N'$. Thus, $\sigma_{N\to N'}(k)$ represents the rotational inelastic cross section for the transition $N \to N'$ as a function of the collision energy, and hence $\sigma^l_{N\to N'}(k)$ stands for the opacity function. Within the IOS framework the state-to-state inelastic cross section can also be expressed as

$$\sigma_{N\to N'}(k) = \sum_{N''=|N'-N|}^{N'+N} (2N'+1) \begin{pmatrix} N' & N'' & N \\ 0 & 0 & 0 \end{pmatrix}^2 \sigma_{0\to N''}(k), \tag{12}$$

where ( ) stands for the $3j$ symbol. This is the so-called factorization formula [31,32].

B. $^2\Sigma$ molecular ion-atom collisions

$^2\Sigma$ molecules are described by Hund's case b, where the the electronic spin S is coupled to the rotational quantum number N, leading to J. The molecular states are labeled $|NSJM\rangle$, M being the projection of J over the quantization axis in the laboratory frame. The scattering of $^2\Sigma$-He can be treated following the approach introduced above, but with $\mathcal{J}$ including the coupling of J with l as shown in detail in Ref. [33]. Within the IOS approximation, it can be shown that the state-to-state cross section is given by [34]

$$\sigma_{NSJ\to N'SJ'}(k) = \sum_\lambda (2N'+1)(2N+1)(2J'+1)$$

$$\times \begin{Bmatrix} \lambda & J & J' \\ S & N' & N \end{Bmatrix}^2 \begin{pmatrix} N' & N & \lambda \\ 0 & 0 & 0 \end{pmatrix}^2 \sigma_{0\to\lambda}(k), \tag{13}$$

where { } represents the $6j$ symbol and

$$\sigma_{0\to\lambda}(k) = \frac{\pi}{k^2} \sum_l \frac{2l+1}{2\lambda+1} |S^l_\lambda(k)|^2 \tag{14}$$

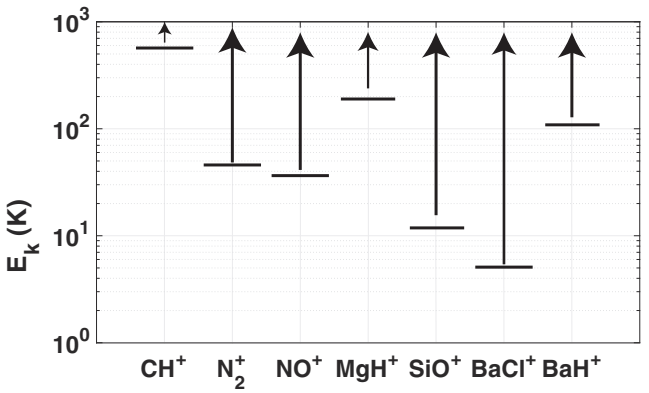

FIG. 3. Validity of the IOS approximation in molecular ion-atom rotational relaxation. Lower bound for the collision energy E_k (in K) in which the IOS approximation holds for different molecular ions in contact with a helium buffer gas.

represents inelastic transitions out of the $N = S = J = 0$ level. Here $S^l_\lambda(k)$ represents the terms of the expansion in a Legendre polynomial basis of the scattering matrix [see Eq. (8)],

$$S^l(k,\delta) = \sum_\lambda S^l_\lambda(k) P_\lambda(\cos\delta). \tag{15}$$

C. Validity of the IOS approximation

Under the IOS approximation for atom-molecule collisions, the molecule does not experience appreciable rotation during the collision with an atom. This physical scenario gets more realistic for high collision energies, as well as for molecules with a small rotational constant, i.e., for heavy molecules. Indeed, one accounts for these effects through the adiabaticity parameter $\xi = \tau_c/\tau_R$ [35], where τ_c and τ_R represent the collisional time and rotational period, respectively. ξ measures the efficiency of the translation-rotational energy transfer; indeed, $\xi \ll 1$ denotes a high energy transfer, whereas $\xi \gg 1$ means a very inefficient energy transfer between the involved degrees of freedom [35]. In the case of molecular ion-atom collisions, the collisional time can be estimated as $\tau_c = b_L/v_{\rm coll}$, where $v_{\rm coll} = \sqrt{2E_k/\mu}$ is the collision velocity for a given collision energy E_k, and $b_L = (2\alpha/(E_k\pi^2))^{1/4}$ stands for the Langevin impact parameter in terms of the polarizability of the atom α. Assuming $N \sim 1$, $\tau_R = B_e^{-1}$, B_e being the rotational constant of the molecular ion, one finds $\xi = B_e b_L/v_{\rm coll}$. Solving this equation for E_k as a function of $\xi \ll 1$ it is possible to estimate the lower bound for E_k, and the results for some molecular ions in a buffer gas of helium are shown in Fig. 3.

The results shown in Fig. 3 indicate that light molecular ions colliding with a buffer gas can only be treated under the IOS approximation at collision energies $\sim$1000 K, as one would expect; however, for heavy molecular ions the lower bound can be below room temperature as is the case for MgH^+ and BaH^+, for instance. Surprisingly, the very interesting $BaCl^+$-He collision can be treated within the IOS framework even at temperatures $\sim$10 K. This may have potential implications in experiments regarding the sympathetic cooling of this molecular ion.

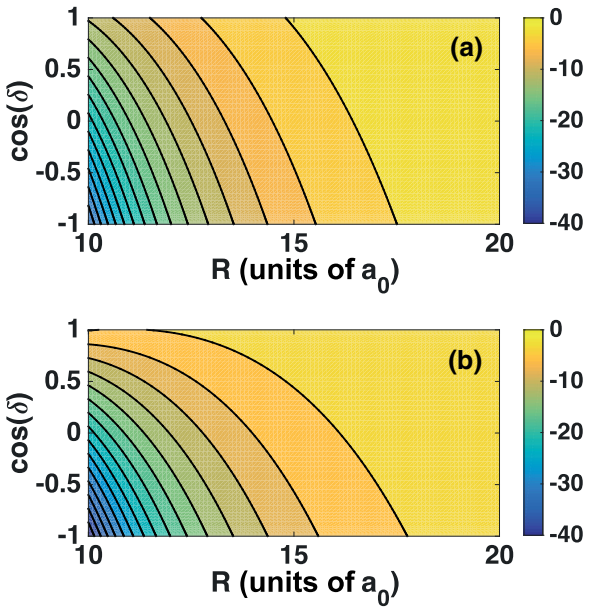

FIG. 4. Potential energy surfaces $V(R,\delta)$ (in K) considered for (a) MgH^+-He and (b) BaH^+-He. R (in a_0) represents the distance between the atom and the CM of the molecular ion, whereas δ (in radians) is the relative angle between **R** and the orientation of the molecule. For these calculations $R_m = 4\ a_0$, and the permanent dipole moments are 3.2 and 5.37 Debye for MgH^+ and BaH^+, respectively [38].

III. RESULTS

The PESs for molecular ion-atom collisions are calculated by means of Eq. (4). The global minimum R_m is taken as 4 a_0 in comparison with the state-of-the-art quantum chemistry calculations in the CH^+-He complex [36,37]. However, the following results are not affected by the choice of of R_m, as pointed out below. The PESs for $(X\ ^1\Sigma)MgH^+$-He and $(X\ ^1\Sigma)$ BaH^+-He are displayed in Fig. 4. This figure shows the expected behavior of the long-range anisotropy based on the $\cos\delta$ dependence and the large influence of the permanent dipole moment of the molecular ion.

A. $^1\Sigma$ ion -He relaxation

Equation (7) including the PES shown in Fig. 4 is solved by the Numerov method for different collision energies $E_k = k^2/(2\mu)$, and its solutions are matched with the boundary condition in Eq. (8), leading to $S^l(k,\delta)$. A radial grid from 2 up to 400 a_0 and a step size $\Delta_R = 0.04\ a_0$ have been employed. Then, $S^l_{0\Omega N'\Omega}$ is obtained by means of Eq. (9), employing 128 points within the Gauss-Legendre quadrature method. Here, we only report on the $0 \to N'$ transitions, since from these processes one can obtain all the state-to-state inelastic cross sections, thanks to the factorization property shown in Eq. (12). $S^l_{0\Omega;N'\Omega}(k)$ is employed for the calculation of the opacity function,

$$\sigma^l_{0\to N'}(k) = \frac{\pi}{k^2}(2l+1)\left|S^l_{00;N'0}(k)\right|^2, \tag{16}$$

and the results are shown in Fig. 5. The opacity functions associated with $0 \to N'$ inelastic collisions, with $N' = 1, 2,$ and 4 are displayed for collision energies of 200 K [Fig. 5(a)] and 300 K [Fig. 5(b)].

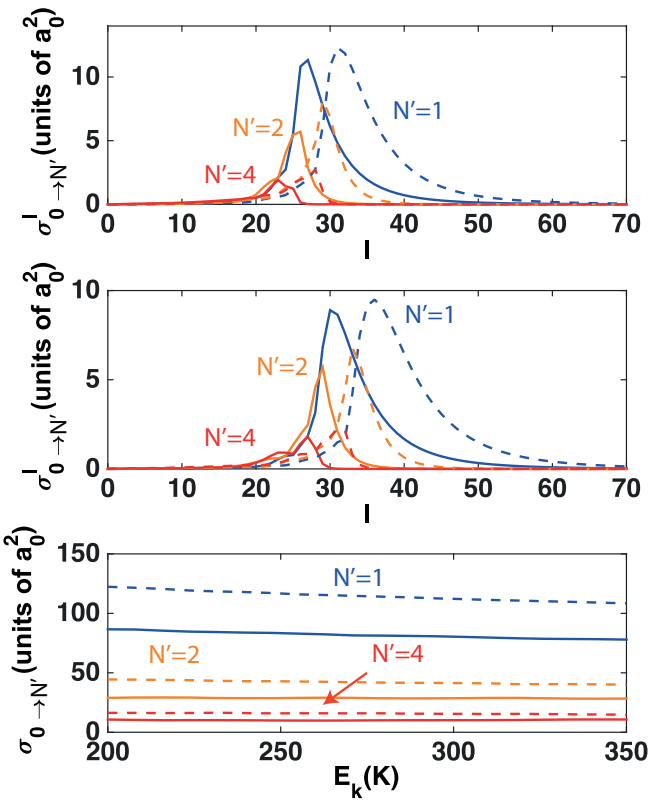

FIG. 5. Rotational relaxation cross section for $^1\Sigma$-He collisions. Opacity functions $\sigma^l_{0\to N'}$ (in a_0^2) for different rotational transitions associated with MgH^+-He (solid lines) and BaH^+-He (dashed lines) are shown for collision energies of (a) 200 K and (b) 300 K. (c) State-to-state cross sections as a function of the collision energy E_k (in K).

Figure 5 shows that the opacity function for a given $0 \to N'$ transition shows a maximum at a given l, hereafter labeled $l_{\rm lmax}$. In this figure it is shown that $l_{\rm lmax}$ is reduced as the rotational excitation involves the exchange of a higher number of rotational quanta, since to observe a larger change in the rotational quanta of the molecular ion, a smaller impact parameter of the atom is needed. The value of $l_{\rm lmax}$ for a given inelastic transition is shifted towards higher l's for higher collision energies as one would expect. And attached to this effect, the distribution of l's with an appreciable contribution to a given transition widens as the collision energy increases. Now we turn to the analysis of the difference between the two collisional systems under study. In this figure, it is shown that the opacity functions associated with BaH^+-He are systematically larger than those associated with MgH^+-He, which is a consequence of the larger permanent dipole moment of BaH^+. But, more interesting with a determined transition and collision energy, the $l_{\rm lmax}$ associated with BaH^+-He is shifted towards higher l's in comparison to that associated with MgH^+-He. This effect can be understood by assuming a capture model (à la Langevin), in which the molecular ion-atom interaction is dominated by the anisotropic-charge-induced dipole term, yielding $l_{\rm max} \sim \sqrt{\mu} d^{1/5} E_k^{3/10}$ and qualitatively explaining the

TABLE I. Close-coupling (CC) versus IOS state-to-state cross section for MgH^+-He and BaH^+-He as a function of the collision energy E_k (in K). The cross section is give in a_0^2.

	MgH^+				BaH^+			
E_k (K)	$\sigma^{CC}_{1\to2}$	$\sigma^{IOS}_{1\to2}$	$\sigma^{CC}_{2\to3}$	$\sigma^{IOS}_{2\to3}$	$\sigma^{CC}_{1\to2}$	$\sigma^{IOS}_{1\to2}$	$\sigma^{CC}_{2\to3}$	$\sigma^{IOS}_{2\to3}$
50	109.10	77.45	–	–	165.95	118.16	82.56	107.63
100	105.32	69.50	83.2	63.81	118.35	105.50	72.56	95.28
200	93.06	65.05	65.81	58.92	100.81	92.21	82.13	83.73
300	73.28	60.48	60.67	55.42	90.42	85.00	80.17	77.02
400	68.92	56.81	55.14	51.84	86.99	80.07	76.56	72.69

results in Fig. 5. However, this model cannot account for the energy-dependent shift associated with the same rotational transition, as one notes comparing $\sigma^{l}_{N\to N'}(k)$ for MgH^+-He (solid line) and BaH^+-He (dashed line) in Figs. 5(a) and 5(b).

To further understand the reliability of the IOS approximation we have solved the close-coupled equations for MgH^+-He, BaH^+-He, and $BaCl^+$-He by means of the hybrid log-derivative-Airy propagator of Alexander and Manolopoulos [39] implemented in MOLSCAT [40]. In particular, for MgH^+-He and BaH^+-He, the propagation has been carried out between 2 a_0 and 400 a_0, including 11 rotational states, i.e., $N_{max} = 10$, guaranteeing a convergence better than 1% in the inelastic cross sections. But, for $BaCl^+$-He, $N_{max} = 14$ is taken and the propagation is carried out between 2 a_0 and 1000 a_0, to reach the same convergence level. The rotational constant for MgH^+ is taken as 6.249 cm^{-1}, whereas the same magnitude is 3.63 and 0.09 cm^{-1} for BaH^+ and $BaCl^+$, respectively. The total angular momentum J of the collision complex is increased until the partial cross sections for the last four consecutive J's each contribute less than 0.02 a_0^2. The results for the state-to-state cross section obtained by solving the coupled-channel equations as well as the IOS cross sections are listed in Table I for MgH^+-He and BaH^+-He. The IOS cross section for each transition has been obtained by means of Eq. (12), and it shows an overall accuracy of 10% and 10%–30% at $E_k = 400$–200 K for BaH^+-He and MgH^+-He, respectively. In the given range of energies the IOS approximation works better for BaH^+-He than for MgH^+-He, since the rotational constant for BaH^+ is smaller than that for MgH^+, as shown in Fig. 3.

In Table II, the IOS state-to-state cross sections for $BaCl^+$-He show an overall accuracy of 5%–25% in comparison with the application of the coupled-channel method to the scattering problem at $E_k = 20$–10 K, as previously anticipated in Fig. 3 using the adiabaticity parameter ξ. However, at 5 K the comparison leads to an error of ∼50%. These calculations confirm that the IOS approximation is a suitable tool for describing the rotational quenching of $BaCl^+$ in a buffer gas of He down to energies of 10 K.

Figure 5(c) displays the state-to-state cross sections for MgH^+-He and BaH^+-He as a function of the collision energy. Here, we note the bigger cross section for BaH^+-He in comparison with MgH^+-He independently of the final state, in correlation with the results regarding the opacity functions in Figs. 5(a) and 5(b). To further compare the rotational relaxation properties of these molecular ions in a buffer gas of helium we have calculated the state-to-state rate coefficients as

$$k_{0\to N'}(T) = \langle v\rangle \beta^2 \int_0^\infty \sigma_{0\to N'}(E_k) E_k e^{-\beta E_k} dE_k, \qquad (17)$$

where $\langle v\rangle = \sqrt{8/(\beta\mu\pi)}$ is the average velocity at a given temperature T and $\beta = (k_B T)^{-1}$, where k_B is the Boltzmann constant. The *down* state-to-state rate coefficients can be calculated by applying the detailed balance condition. The results are listed in Table III, where it is observed that BaH^+-He has a relaxation rate coefficient 33% larger than that of MgH^+-He. We have confirmed that our results do not depend drastically on the choice of R_m; indeed changing R_m by 1 a_0 affects the results by less than 5%. In particular, assuming typical He buffer gas densities of 10^{15} cm^3, and taking into account $k_{0\to N'}(T) \sim 10^{-10}$ $cm^3\,s^{-1}$, one finds that molecular ions experience one collision per microsecond, which is faster than the typical radiative decay time of molecular ions, ∼1 ms. Therefore, collisional relaxation processes may be useful for rotational cooling protocols of ions immersed in a Paul trap.

From the state-to-state rate coefficients in Table III we have obtained a general expression for the rates as a function of the

TABLE II. Close-coupling (CC) versus IOS state-to-state cross section for $BaCl^+$-He as a function of the collision energy E_k (in K). The cross section is given in a_0^2. For these calculations $BaCl^+$-He PES is modeled following Eq. (4), with $R_m = 6.45\ a_0$, which corresponds with the global minimum for the $BaCl^+$-Ca interaction [13]. The dipole moment of $BaCl^+$ is taken as 8.927 Debye [13].

E_k (K)	$\sigma^{CC}_{1\to2}$	$\sigma^{IOS}_{1\to2}$	$\sigma^{CC}_{2\to3}$	$\sigma^{IOS}_{2\to3}$
20	218.01	202.82	206.34	185.79
15	230.15	209.79	223.08	188.32
10	260.04	222.97	264.79	199.73
5	406.60	232.85	336.43	217.48

TABLE III. State-to-state rate coefficients for MgH^+-He and BaH^+-He as a function of the temperature T (in K). Rates are in units of 10^{-10} $cm^3\,s^{-1}$.

	MgH^+				BaH^+			
T	$k_{0\to1}$	$k_{0\to2}$	$k_{0\to3}$	$k_{0\to4}$	$k_{0\to1}$	$k_{0\to2}$	$k_{0\to3}$	$k_{0\to4}$
150	3.00	1.02	0.56	0.37	4.04	1.45	0.80	0.52
200	3.28	1.14	0.63	0.42	4.38	1.59	0.88	0.57
250	3.50	1.23	0.68	0.45	4.63	1.69	0.93	0.61
300	3.64	1.29	0.72	0.47	4.80	1.76	0.98	0.64

dipole moment of the molecular ion and the temperature of the buffer gas,

$$k_{0\to N'}(T) = \frac{A_{N'}\sqrt{d}}{(k_B T)^{0.22}}\langle v\rangle\sqrt{\frac{\mu}{\mu_{\mathrm{BaH}}}}, \tag{18}$$

where $A_{N'}$ is a fit parameter ($A_{N'}\sqrt{d}$ has units of length^4 time^{-2} $\times$ mass) that depends on the final state, d is the permanent dipole moment of the molecular ion in atomic units, μ stands for the reduced mass of the colliding molecular ion-atom in atomic units, and μ_{BaH} is the same magnitude, but for the particular case of BaH^+-He, $k_B T$ must be given in atomic units as well as $\langle v\rangle$, and hence $k_{0\to N}(T)$ in Eq. (18) is in atomic units. In particular, we find $A_1 = 20.26 \pm 0.30$, $A_2 = 7.35 \pm 0.2$, $A_3 = 4.07 \pm 0.05$, and $A_4 = 2.65 \pm 0.03$, leading to an overall error of 5% in comparison with the full numerical simulations. Equation (18) depends on the permanent dipole moment of the molecular ion as $\sqrt{d}$, which is very similar to our results based on a capture model $d^{1/5}$. This dependence implies that the systems studied in this section are not in a perturbative regime, where the expected d^2 should appear. Equation (18) can be applied to any polar $^1\Sigma$ ion-He collision for 150 K $\leqslant$ T $\leqslant$ 400 K.

In principle, one can assume that the inelastic rate coefficient might be of the same order of magnitude as the Langevin rate coefficient, which only accounts for the $\alpha R^{-4}/2$ long-range interaction and it is independent of the temperature. The Langevin rate coefficients for the system studied in this section are 5.7×10^{-10} cm^3 s^{-1} and 5.4×10^{-10} cm^3 s^{-1} for BaH^+-He and MgH^+-He, respectively. Comparing these numbers with the results listed in Table III, the Langevin rate coefficient is larger than the accurate inelastic rate coefficient for the exchange of a single rotational quantum by a factor of 2 in the range 150 K $\leqslant$ T $\leqslant$ 300 K. However, the comparison is worst for state-to-state processes involving the exchange of two or more rotational quanta, observing deviations up to one order of magnitude. This deviation is a consequence of the influence of the dipole moment of the molecular ion leading to an extra long-range tail $\propto R^{-5}$, which plays a role in the rotational dynamics.

B. $^2\Sigma$ ion–He relaxation

Here, we present the results for the rotational relaxation associated with SiO^+-He. As in the previous section, $S^l(k,\delta)$ is obtained by solving Eq. (7) for different collision energies E_k and partial waves l and matching with the proper scattering boundary conditions. Then, by means of Eq. (15) and taking into account the orthogonality relations for the Legendre polynomials, one finds

$$S^l_\lambda(k) = \frac{2\lambda+1}{2}\int_0^\pi S^l(k,\delta)P_\lambda(\cos\delta)\sin\delta d\delta, \tag{19}$$

which is numerically implemented by employing 128 Gauss-Legendre quadrature points. Next, following Eq. (14) one computes the energy-dependent state-to-state inelastic transitions out of the $N = J = S = 0$ state $\sigma_{0\to\lambda}(k)$, where $\lambda = 1,2,\ldots,q$ represents a rotational transition to $N' = 1,2,\ldots,q$, and the results are shown in Fig. 6. In this figure it is shown that the state-to-state cross section for $\lambda = 1$ shows the largest value, followed by $\lambda = 2$ and $\lambda = 4$. This trend shows the influence of the anisotropy of the underlying PES at the energy range explored here; in particular, it implies that in the Legendre expansion of the PES $V(R,\delta)$ the dominant term will be the linear one, followed by the second one, and so on. In Fig. 6 the results for $\lambda \neq 1$ show some undulations that we attribute to the short-range physics and hence are classified as glory undulations.

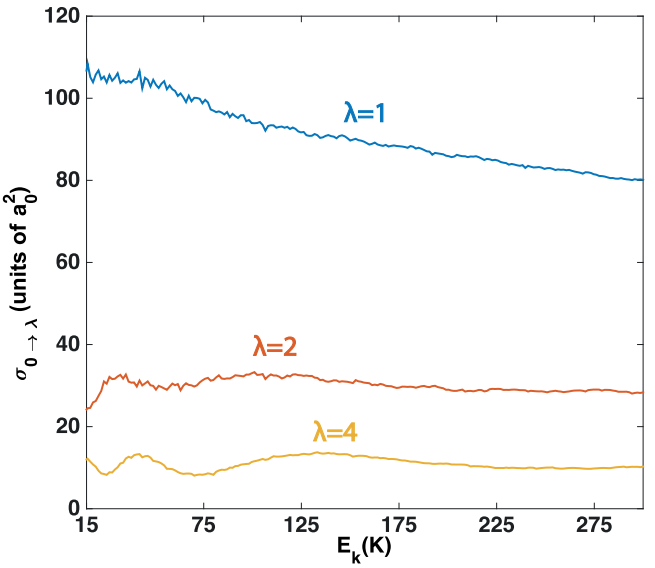

FIG. 6. State-to-state rotational relaxation cross section (in a_0^2) out of the $N = J = S = 0$ state for $SiO^+(^2\Sigma)$-He collisions as a function of the collision energy E_k (in K). The permanent dipole moment for SiO^+ taken in these calculations is 3.0982 Debye.

The most appropriate physical magnitude to account for relaxation is the state-to-state rate coefficient, which in the present case—thanks to the linear properties of the integral operator—allows us to define it as

$$k_{NSJ\to N'SJ'}(T) = \sum_\lambda (2N'+1)(2N+1)(2J'+1) \times \begin{Bmatrix} \lambda & J & J' \\ S & N' & N \end{Bmatrix}^2 \begin{pmatrix} N' & N & \lambda \\ 0 & 0 & 0 \end{pmatrix}^2 k_{0\to\lambda}(T), \tag{20}$$

where the state-to-state rate coefficient out of the $N = J = S = 0$ state is given by

$$k_{0\to\lambda}(T) = \langle v\rangle\beta^2\int_0^\infty \sigma_{0\to\lambda}(E_k)E_k e^{-\beta E_k}dE_k. \tag{21}$$

The results of $k_{0\to\lambda}(T)$ for different temperatures are listed in Table IV, where all the rate coefficients show a similar trend with respect to the temperature, in accordance with the results for other atom-molecule collisions listed in Table III. In this table it is shown that the influence of the $0 \to 4$ transition is one order of magnitude smaller than that of the $0 \to 1$, thus only including up to $\lambda = 4$ is enough to have a satisfactory description of the state-to-state rate coefficient. From the results listed in Table IV it is possible to calculate any state-to-state rate coefficient from Eq. (20) by taking into account the proper angular momentum algebra throughout the $3j$ and $6j$ symbols.

TABLE IV. State-to-state rate coefficients for SiO^+-He as a function of the temperature T (in K). Rates are in units of 10^{-10} cm^3 s^{-1}.

T	$k_{0\to1}$	$k_{0\to2}$	$k_{0\to3}$	$k_{0\to4}$
50	1.45	0.46	0.24	0.16
100	1.89	0.63	0.35	0.23
150	2.17	0.75	0.42	0.28
200	2.39	0.84	0.47	0.32
250	2.57	0.92	0.52	0.36
300	2.72	0.98	0.56	0.38

The results listed in Table IV are more attractive if we show them as a function of the temperature,

$$k_{0\to\lambda}(T) = \frac{A_\lambda\sqrt{d}}{(k_B T)^{\xi_\lambda}}\langle v\rangle, \tag{22}$$

where A_λ is a fit parameter (having the same units as $A_{N'}$) that depends on the final state, ξ_λ is a free parameter, and hence $k_{0\to\lambda}(T)$ in Eq. (22) is in atomic units. In particular, we find $A_1 = 23.74 \pm 0.2$, $\xi_1 = 0.15 \pm 0.2$, $A_2 = 13.95 \pm 0.2$, $\xi_2 = 0.08$, $A_3 = 11.36 \pm 0.2$, $\xi_3 = 0.03$, $A_4 = 8.92 \pm 0.2$, and $\xi_4 = 0.01$, leading to an overall error of 5% in comparison with the full numerical simulations. Equation (22) can be applied to any polar $^2\Sigma$ ion–He collision for 15 K $\leqslant T$.

For this molecular ion-atom collision the Langevin rate coefficient is 5.5×10^{-10} cm^3 s^{-1}, which is a factor of two or three times larger than the one obtained in the present simulations for the exchange of one rotational quanta and one order of magnitude larger than transitions regarding exchange of multiple rotational quanta. This difference, as well as the deviation presented in the previous section, is due to the influence of the R^{-5} potential, since it plays an important role in the range of collision energies studied in this work, thus showing the influence of the dipole moment of the molecular ion at hand.

IV. CONCLUSIONS

In the present work, the IOS approximation has been reviewed and applied to the study of the rotational inelastic cross section for $^1\Sigma$ and $^2\Sigma$ molecular ion–He collisions. In particular, we have presented a study of the state-to-state rate coefficient for MgH^+-He and BaH^+-He from 150 to 300 K, whereas SiO^+-He collisions have been studied from 15 to 300 K, the range of validity of the IOS approximation in those collisions. From the state-to-state rate coefficients and based on a capture model we propose a pseudoempirical expression for the rate coefficient in terms of the temperature and the permanent dipole moment of the molecular ion d, which weakly depends on T but is proportional to $\sqrt{d}$. The obtained functional form is applicable to all $^1\Sigma$ and $^2\Sigma$ heteronuclear molecular ions colliding with He. As a result, the rotational relaxation mechanism in BaH^+-He is 25% more efficient than that in MgH^+. Therefore, BaH^+ seems to be a very good candidate for rotational relaxation of molecular ions in contact with a buffer gas. In a similar vein, the study of SiO^+-He shows a comparable state-to-state rate coefficient to MgH^+-He, thus it is a fairly good candidate for collisional-assisted rotational cooling.

The range of applicability of the IOS approximation has been explored for several molecular ions of interest in cold chemistry experiments. In particular, by comparing the IOS state-to-state cross section with respect to the coupled-channel method, it is found that it may be valid down to collision energies of $\sim$100 K in the case of BaH^+-He, with an error of $\lesssim$20%, and for MgH^+-He at $\sim$200 K the error is $\lesssim$25%. In the case of $BaCl^+$-He the IOS approach gives fairly accurate inelastic cross sections down to energies of $\sim$10 K, with an error of $\lesssim$25%. These very encouraging results may have important applications in the theoretical study of rotational relaxation of molecular ions in contact with a buffer gas. Finally, it is worth emphasizing that the IOS approximation presents the opportunity of obtaining fairly accurate state-to-state cross sections with just a handful of inelastic cross sections starting at $N = 0$. Thus, characterizing the energy dependence of these brings an intuitive way to characterize the state-to-state cross sections, which is not possible with the more accurate but complex close-coupled approach to the problem.

ACKNOWLEDGMENTS

We thank Brian Odom and Pat Stollenwerk for helpful and elucidating discussions as well as for careful reading of the manuscript. This material is based upon work supported by the National Science Foundation under Grant No. 1404419-PHY.

[1] F. H. J. Hall, M. Aymar, N. Bouloufa-Maafa, O. Dulieu, and S. Willitsch, Phys. Rev. Lett. **107**, 243202 (2011).
[2] F. H. J. Hall, P. Eberle, G. Hegi, M. Raoult, M. Aymar, O. Dulieu, and S. Willitsch, Mol. Phys. **111**, 2020 (2013).
[3] F. H. J. Hall, M. Aymar, M. Raoult, O. Dulieu, and S. Willitsch, Mol. Phys. **111**, 1683 (2013).
[4] A. Härter and J. H. Denschlag, Contemp. Phys. **55**, 33 (2014).
[5] L. Ratschbacher, C. Zipkes, C. Sias, and M. Köhl, Nat. Phys. **8**, 649 (2012).
[6] W. W. Smith, D. S. Goodman, I. Sivarajah, J. E. Wells, S. Baberjee, R. Côté, H. H. Michels, J. A. Mongtomery, and F. A. Narducci, Appl. Phys. B **112**, 75 (2014).
[7] S. Willitsch, M. T. Bell, A. D. Gingell, and T. P. Softley, Phys. Chem. Chem. Phys. **10**, 7200 (2008).
[8] C. Zipkes, S. Palzer, L. Ratschbacher, C. Sias, and M. Köhl, Phys. Rev. Lett. **105**, 133201 (2010).
[9] A. Krükow, A. Mohamadi, A. Härter, J. H. Denschlag, J. Pérez-Ríos, and C. H. Greene, Phys. Rev. Lett. **116**, 193201 (2016).
[10] F. H. J. Hall and S. Willitsch, Phys. Rev. Lett. **109**, 233202 (2012).
[11] E. R. Hudson, Phys. Rev. A **79**, 032716 (2009).
[12] A. K. Hansen, O. O. Versolato, L. Klosowski, S. B. Kristensen, A. Gingell, M. Schwartz, A. Windberger, J. Ullrich, J. R. C. López-Urrurita, and M. Drewsen, Nature **508**, 76 (2014).

[13] T. Sotecklin, P. Halvick, M. A. Gannouni, M. Holchaf, S. Kotochigova, and E. R. Hudson, Nat. Commun. **7**, 11234 (2016).
[14] K. Chen, S. J. Showalter, S. Kotochigova, A. Petrov, W. G. Rellergert, S. T. Sullivan, and E. R. Hudson, Phys. Rev. A **83**, 030501(R) (2011).
[15] J. Mur-Petit, J. J. García-Ripoll, J. Pérez-Ríos, J. Campos-Martínez, M. I. Hernández, and S. Willitsch, Phys. Rev. A **85**, 022308 (2012).
[16] D. Leibfired, New. J. Phys. **14**, 023029 (2012).
[17] F. Wolf, Y. Wang, J. C. Heip, F. Gebert, C. Shi, and P. O. Schmidt, Nature **530**, 457 (2016).
[18] J. O. Hirschfelder, C. F. Curtiss, and R. B. Bird, *Molecular Theory of Transport in Gases* (Wiley, New York, 1954).
[19] F. R. W. McCourt, J. J. M. Beenakker, W. E. Köhler, and I. Kuscer, *Nonequilibrium Phenomena in Polyatomic Gases*, Vol. 2 (Clarendon Press, Wotton-under-Edge, UK, 1991).
[20] V. M. Zhdanov, *Transport Processes in Multicomponent Plasma* (Taylor and Francis, London, 2002).
[21] S. Montero and J. Pérez-Ríos, J. Chem. Phys. **141**, 114301 (2014).
[22] P. McGuire, Chem. Phys. Lett. **23**, 575 (1973).
[23] P. McGuire and D. J. Kouri, J. Chem. Phys. **60**, 2488 (1974).
[24] T. P. Tsien and T. R. Pack, Chem. Phys. Lett. **6**, 54 (1970).
[25] T. P. Tsien and T. R. Pack, Chem. Phys. Lett. **8**, 579 (1971).
[26] T. R. Pack, Chem. Phys. Lett. **13**, 393 (1972).
[27] T. P. Tsien, G. A. Parker, and T. R. Pack, J. Chem. Phys. **59**, 5373 (1973).
[28] D. Secrest, J. Chem. Phys. **62**, 710 (1975).
[29] A. M. Arthurs and A. Dalgarno, Proc. Roy. Soc. A **256**, 540 (1960).
[30] D. Flower, *Molecular Collisions in the Interestellar Medium*, edited by D. Flower (Cambridge University Press, Cambrige, UK, 2007).
[31] H. J. Korsch and A. Ernesti, J. Phys. B **25**, 3565 (1992).
[32] S. Goldflam, R. Green, and D. J. Kouri, J. Chem. Phys. **67**, 4149 (1977).
[33] M. H. Alexander, J. Chem. Phys. **76**, 3637 (1982).
[34] G. C. Corey and F. R. McCourt, J. Phys. Chem. **87**, 2723 (1983).
[35] R. D. Levine and R. B. Bernstein, *Molecular Reaction Dynamics and Chemical Reactivity* (Oxford University Press, Oxford, UK, 1987).
[36] K. Hammami, L. C. O. Owono, N. Jaidane, and Z. B. Lakhdar, J. Mol. Struct. TEOCHEM **853**, 18 (2008).
[37] T. Soecklin and A. Voronin, Eur. Phys. J. D **46**, 259 (2008).
[38] M. Abe, M. Kajita, M. Hada, and Y. Moriwaki, J. Phys. B **43**, 245102 (2010).
[39] M. H. Alexander and D. E. Manolopoulos, J. Chem. Phys. **86**, 2044 (1987).
[40] J. M. Hutson and S. Green, MOLSCAT, Collaborative Computational Project No. 6 of the UK Science and Engineering Research Council, Version 14 (1994).